Published in final edited form as:
Neuron. 2012 February 9; 73(3): 482–496. doi:10.1016/j.neuron.2011.11.021.

Palmitoylation by DHHC5/8 targets GRIP1 to dendritic endosomes to regulate AMPA-R trafficking

Gareth M. Thomas[1], **Takashi Hayashi**[2], **Chih-Ming Chen**, **Shu-Ling Chiu**[3], and **Richard L. Huganir**[*]
Department of Neuroscience and Howard Hughes Medical Institute Johns Hopkins University School of Medicine Hunterian 1001 725 N Wolfe Street Baltimore, MD 21205 USA

Summary

Palmitoylation, a key regulatory mechanism controlling protein targeting, is catalyzed by DHHC-family palmitoyl acyltransferases (PATs). Impaired PAT activity is linked to several neurodevelopmental and neuropsychiatric disorders, suggesting critical roles for palmitoylation in neuronal function. However, few substrates for specific PATs are known, and functional consequences of specific palmitoylation events are frequently uncharacterized. Here, we identify two related PATs, DHHC5 and DHHC8, as specific regulators of the PDZ domain protein GRIP1b. Binding, palmitoylation and dendritic targeting of GRIP1b require a DHHC5/8 PDZ ligand that is absent in all other PATs. Palmitoylated GRIP1b is targeted to trafficking endosomes, and may link endosomes to kinesin motors. Consistent with this trafficking role, GRIP1b's palmitoylation turnover rate approaches the highest of all reported proteins, and palmitoylation increases GRIP1b's ability to accelerate AMPA-R recycling. These findings identify the first neuronal DHHC5/8 substrate, define novel mechanisms controlling palmitoylation specificity, and suggest further links between dysregulated palmitoylation and neurodevelopmental / neuropsychiatric conditions.

Introduction

Precise targeting of proteins to specific subcellular locations is critical in all cells, but its importance is especially apparent in highly specialized, polarized cells such as neurons. Neuronal protein targeting must be precisely regulated to control neurotransmission at specific synapses, which in turn underlies higher brain functions such as synaptic plasticity, learning and memory (Shepherd and Huganir, 2007; Newpher and Ehlers, 2008, Lau and Zukin, 2005).

A major mechanism that controls protein targeting to specific subcellular locations is direct lipid modification, which facilitates protein interactions with intracellular or plasma membranes (Johnson et al., 1994; Zhang and Casey, 1996; El-Husseini and Bredt, 2002;

[*]Corresponding author: rhuganir@jhmi.edu.
[1]Current addresses: Shriners Hospital Pediatric Research Center (Center for Neurorehabilitation and Neural Repair), Temple University Medical School, 3500 N. Broad Street, Philadelphia, PA 19130
[2]Department of Molecular Neurobiology and Pharmacology, Graduate School of Medicine, The University of Tokyo, 7-3-1 Hongo, Bunkyo-ku, Tokyo 113-0033, Japan
[3]Graduate Program, Department of Biology, Johns Hopkins University, 3400 N. Charles St., 224 Mudd Hall, Baltimore, MD 21218

Fukata and Fukata, 2010). Of the three most common lipid modifications, myristoylation, prenylation and palmitoylation, only palmitoylation is reversible. This allows additional dynamic regulation and may be one reason why palmitoylation is more frequently observed in neurons than other lipid modifications (Fukata and Fukata, 2010). Indeed, palmitoylation is rapidly emerging as a critical modulator of neuronal function, whose disruption is linked to neurodevelopmental and neuropsychiatric conditions (Fukata and Fukata, 2010; Mukai et al., 2004; Mukai et al., 2008; Mansouri et al., 2005; Raymond et al., 2007).

In mammalian cells, palmitoylation is catalyzed by a family of palmitoyl acyltransferases (PATs), each containing a conserved Asp-His-His-Cys (DHHC) motif (Fukata et al., 2004). Many PATs are expressed in neurons (Heiman et al., 2008; Doyle et al., 2008), but two PATs, DHHC5 and DHHC8, are detected far more frequently than others at both the mRNA and protein levels in neuronal studies (Trinidad et al., 2006; Trinidad et al, 2008; Munton et al., 2007; Heiman et al., 2008; Doyle et al., 2008). This suggests that DHHC5/8 might be particularly important in neuronal regulation. Consistent with this hypothesis, DHHC5 is implicated in higher brain function, since mice with reduced DHHC5 levels (a hypomorphic `gene trap' line) show impaired performance in a learning task (Li et al., 2010). Moreover, neurons from DHHC8 knockout mice have a reduced density of dendritic spines and glutamatergic synapses (Mukai et al., 2008). In addition to their physiological roles, both DHHC5 and DHHC8 are linked to neuropsychiatric conditions. The *ZDHHC5* gene, which codes for DHHC5, lies in a region of Chromosome 11 associated with bipolar disorder (Fallin et al. 2004), while the *ZDHHC8* gene lies in a region of Chromosome 22 repeatedly implicated in schizophrenia (Mukai et al. 2004; Chen et al., 2005). Palmitoylation of neuronal proteins by DHHC5/8 is therefore likely essential for normal neuronal function and may be impaired in disease states. However, little is known regarding the direct neuronal substrates of DHHC5/8.

Here we identify a specific splice form of the multi-PDZ domain containing protein GRIP1b as a novel neuronal substrate for DHHC5/8. Palmitoylated GRIP1b, which is targeted to trafficking endosomes, serves as a specific link between endosomes and microtubule motors. This localization places palmitoylated GRIP1b in a perfect position to mediate activity-dependent AMPA-R trafficking, a role we recently revealed for GRIP1. Indeed, palmitoylation enhances GRIP1b's ability to accelerate AMPA-R recycling. Strikingly, binding, palmitoylation and dendritic targeting of GRIP1b by DHHC5 all require a novel PDZ ligand-dependent recognition mechanism. These findings not only identify the first neuronal DHHC5/8 substrate but also define novel mechanisms controlling palmitoylation specificity.

Results

DHHC5 and DHHC8 bind and palmitoylate GRIP1b

DHHC5 and 8 are closely related, but differ markedly in structure from all other PATs because they possess greatly extended C-terminal tails (Fukata et al., 2004; Ohno et al., 2006). We hypothesized that these tails might provide clues to the possible specific roles and targets of DHHC5/8. In particular, we noticed that both tails end with a motif that is predicted to bind to PDZ domain-containing proteins (Kim and Sheng, 2004;Feng and Zhang, 2009). PDZ domain proteins are heavily implicated in many aspects of neuronal regulation, but are especially known to control the targeting and trafficking of glutamate receptors (Kornau et al., 1995; Dong et al., 1997; Srivastava et al., 1998; Steinberg et al., 2006; Daw et al., 2000; Osten et al., 2000; Wyszinski et al., 2002; Terashima et al., 2008; Hanley, 2008). We therefore hypothesized that DHHC5/8 might use their C-terminal motif to bind specific PDZ domain proteins and potentially to recognize them as substrates for palmitoylation.

The DHHC5 and DHHC8 C-termini are identical and conform to a Type II PDZ ligand (EISV; Fig1A, Songyang et al., 1997). As a first step to address the possibility that DHHC5/8 use this C-terminal motif to bind specific substrates, we performed a yeast two-hybrid screen of a rat hippocampal cDNA library using a C-terminal bait that included the shared DHHC5/8 PDZ ligand. Of 8×10^6 clones screened, four `hits' encoded an identical central region (PDZ domains 4 thru 6: `GRIP1–456') of the multi-PDZ domain adaptor protein GRIP1 (Dong et al., 1997). Consistent with the fact that their PDZ ligands are identical, GST fusions of both DHHC5 and DHHC8 C-termini bound robustly to GRIP1–456 in co-transfected HEK293T cells. No binding of GRIP1–456 was observed with GST alone, or with DHHC5 or DHHC8 C-termini lacking the PDZ ligand (Fig1B, C). PDZ ligand-dependent binding of both DHHC5 and DHHC8 C-terminal tails was also observed when the experiment was performed in the reverse direction (to detect DHHC5/8 tails in myc-GRIP1–456 immunoprecipitates (Fig S1A, B). Moreover, the shared DHHC5/8 C-terminal 15AA sequence was sufficient to robustly bind GRIP1–456 (Fig S1C).

Alternative splicing produces two GRIP1 isoforms, GRIP1a and GRIP1b, which differ in a unique N-terminal sequence (Fig 1D; Yamazaki et al., 2001). It was previously reported that GRIP1b is specifically palmitoylated, although the PAT(s) responsible was not identified (Yamazaki et al., 2001). To test whether DHHC5 and/or DHHC8 specifically palmitoylate GRIP1b, we optimized a non-radioactive acyl-biotinyl exchange (ABE) assay (Hayashi et al., 2009; Wan et al., 2007; Drisdel et al, 2006). ABE is a chemical exchange of biotin for thioester-linked acyl modifications (i.e. palmitoylation), with the resulting biotinylated protein being affinity-purified by neutravidin agarose. ABE avoids the long exposure times required for [^{3}H]-palmitate incorporation experiments and was used routinely for this study, although major findings were also shown by [^{3}H]-palmitate incorporation, with essentially identical results (Fig S1D and main Fig 2E).

GRIP1b expressed in HEK293T cells was significantly palmitoylated, as detected by ABE, but GRIP1b palmitoylation was robustly increased by co-expression of either DHHC5 or DHHC8 (Fig 1E, F). In contrast, the GRIP1a splice variant was not palmitoylated, either when expressed alone, or with DHHC5 or DHHC8 (Fig 1E, F). Because GRIP1a differs from GRIP1b only at its N-terminus (Fig 1F), this suggested that DHHC5 and DHHC8 specifically palmitoylate the unique N-terminal Cysteine, Cys11, of GRIP1b. Indeed, point mutation of GRIP1b Cys11 to a non-palmitoylatable serine abolished palmitoylation by DHHC5 and DHHC8 (not shown).

We next examined the ability of specific DHHC5/8 mutants to palmitoylate GRIP1b. As expected, GRIP1b was not palmitoylated by catalytically inactive PAT mutants (catalytic Cys mutated to Ser; DHH**S**5, DHH**S**8; Fig 1G, H). Strikingly, GRIP1b was also not palmitoylated by DHHC5 and DHHC8 mutants lacking the C-terminal PDZ ligand (Fig 1G, H). Quantification of palmitoylated:total GRIP1 levels from multiple experiments confirmed these results (Fig S1E, F). These findings suggest that DHHC5/8 can bind and palmitoylate GRIP1b in heterologous cells, and require both catalytic activity and PDZ domain binding to recognize GRIP1 as a substrate.

DHHC5 is a major neuronal PAT for GRIP1b

Little is known regarding the endogenous subcellular distribution of DHHC5 and DHHC8 and their specific roles in neurons. To gain insight into whether DHHC5 and/or DHHC8 palmitoylate GRIP1 in neurons, we first used specific antibodies (Fig S2A) to immunolocalize these two PATs. Both DHHC5 and DHHC8 were clearly detected in dendrites (Fig 2A). DHHC8 was largely synaptically localized, as shown by colocalization with the synaptic active zone protein Bassoon (Fig 2A). In contrast, DHHC5 colocalized only rarely with Bassoon, but was strongly detected within dendritic shafts (Fig 2A). To

confirm DHHC5 distribution, we also expressed epitope-tagged DHHC5 in hippocampal neurons. Both Myc- and HA-tagged DHHC5 immunostaining mirrored the pattern seen for endogenous DHHC5, being detected occasionally in dendritic spines, but frequently in dendritic shafts (Fig 2B, Fig S2B). Consistent with this distribution, myc-DHHC5 puncta colocalized only occasionally with the synaptic marker PSD-95 (Fig 2B).

This extensive dendritic distribution of DHHC5 and DHHC8 contrasted markedly to the ER / Golgi localization reported for many other PATs (Ohno et al., 2006). To further explore this difference, we compared DHHC5 distribution with two other PDZ ligand-containing PATs, DHHC3 and DHHC7. Both DHHC3 and DHHC7 localized exclusively with a Golgi marker (Fig S2B) and were absent from dendrites, and quantitative comparison of DHHC3 and DHHC5 dendritic distribution confirmed this highly significant difference (Fig S2C). DHHC5 signals also extended far beyond the somatic signal seen with the ER marker KDEL-CFP (Fig S2D). Together, these data suggest that DHHC5 and DHHC8 are present in dendritic locations in neurons that differ from other PATs, where they may play unique roles.

Biochemical analysis of DHHC5 and DHHC8 distribution supported these immunostaining data: DHHC8 was enriched in post-synaptic density (PSD) fractions, consistent with its synaptic localization, while DHHC5, though detectable in PSD fractions, was markedly less enriched, consistent with its more prominent dendritic distribution (Fig 2C). Fidelity of the PSD preparation was confirmed by immunoblotting with pre and post-synaptic markers (Fig S2E).

The dendritic localization of DHHC5 resembles the previously reported distribution of GRIP1, which is present throughout dendritic shafts, but only rarely in dendritic spines (Wyszinski et al., 1999; Mao et al., 2010, Fig 2D). However, previous reports of GRIP1 localization did not distinguish between GRIP1a and GRIP1b. We therefore developed a GRIP1b-specific antibody (characterized in Fig S2F). The GRIP1b antibody recognized numerous dendritic puncta (Fig 2D), which resembled the previous reported distribution of GRIP1 (Mao et al., 2010) and overlapped almost entirely with signal detected by a pan-GRIP1 monoclonal antibody (Fig 2D). By contrast, GRIP1b colocalized with neither the synaptic marker PSD-95 (Fig S2G) nor the Golgi marker GM130 (Fig S2H). Together, these data suggest that GRIP1b is largely present in dendritic puncta, similar to DHHC5. Biochemical data also supported this conclusion, as subcellular distribution of both GRIP1 and GRIP1b was broadly similar to DHHC5 (Fig S2E).

Although GRIP1b is palmitoylated in heterologous cells, endogenous GRIP1 palmitoylation is not well characterized in neurons. Using [^{3}H]-palmitate labeling, we first confirmed that GRIP1 is indeed palmitoylated in primary neurons (Fig 2E). Immunoblotting of ABE samples with a `pan-GRIP1' antibody also showed a robust signal, confirming GRIP1 palmitoylation in both cultured neurons and in intact brain (Fig 2E). To specifically detect GRIP1b palmitoylation, we probed the same ABE samples with our GRIP1b antibody. Strikingly, this suggested a higher percentage of GRIP1b is palmitoylated in neurons than the well-known palmitoyl-protein PSD-95 (Fig 3A).

Their similar subcellular localization suggests that DHHC5 is appropriately positioned to palmitoylate GRIP1b in neurons. Indeed, although GRIP1b protein was detected as early as DIV5 (Fig 2F), GRIP1b palmitoylation was detected only at later times (DIV12-19), coincident with the appearance of DHHC5 (Fig 2F). Moreover, neurons infected with lentivirus encoding a short hairpin RNA (shRNA) that specifically targets DHHC5 (Fig S2I) showed markedly reduced levels of palmitoylated, but not total, GRIP1 (Fig 2G, H). Importantly, as a control for potential off-target effects of shRNA, both DHHC5 levels and

GRIP1 palmitoylation were rescued by co-expression of shRNA-resistant DHHC5 (Fig 2G, H). DHHC5 knockdown and rescue did not affect either palmitoylated or total levels of the known palmitoyl proteins Fyn (Fig 2G) or SNAP25 (not shown).

DHHC5 knockdown did not completely eliminate GRIP1b palmitoylation, suggesting that other PATs, in particular DHHC8, might compensate for loss of DHHC5. Indeed, while infection of a DHHC8-specific (Fig S2J, S2K) shRNA only slightly reduced GRIP1 palmitoylation, co-infection with shRNAs targeting DHHC5 and DHHC8 together reduced GRIP1 palmitoylation to almost undetectable levels (Fig 2G, H). Levels of total and palmitoylated SNAP25 and Fyn were unaffected, even in DHHC5 plus DHHC8 knockdown neurons. These results strongly suggest that both DHHC5 and DHHC8 can palmitoylate GRIP1 in neurons, but that DHHC5 is the major endogenous regulator of GRIP1 palmitoylation. Indeed, an antibody that recognizes both DHHC5 and DHHC8 equally revealed that DHHC5 is by far the major of these two PATs in our neuronal cultures (Fig S2L). Thus, in subsequent experiments we focused our attention on DHHC5.

Rapid GRIP1b palmitate turnover suggests a role in dynamic trafficking

Although palmitoylation is reversible, rates of palmitate turnover on neuronal proteins vary widely (Huang and El-Husseini, 2005; Kang et al., 2008). Palmitate turnover rate can provide insight into the possible function of palmitoylation; rapid turnover suggests a role in dynamic events such as regulated protein trafficking, while slow palmitate turnover suggests a role in long-term static protein targeting. As a first step to address the functional consequence of GRIP1b palmitoylation, we determined the palmitate turnover rate of GRIP1. Treating neurons with the broad-spectrum palmitoylation inhibitor 2-Bromopalmitate, which blocks palmitate addition (Webb et al., 2000; Resh, 2006) allows palmitate turnover rate to be measured by tracking kinetics of palmitoylation `run down' in ABE samples. Strikingly, almost all palmitate on GRIP1 was removed after only 1 hour of 2-Bromopalmitate treatment (Fig 3A). Indeed, GRIP1 palmitate cycling was faster (T1/2 approx. 35 min, Fig 3B) than any other protein that we examined, including the well known reversibly palmitoylated protein PSD-95 (El-Husseini et al., 2002; Fig 3A, B) and approaches the fastest turnover rates reported for any known palmitoyl-protein (Magee et al., 1987; Rocks et al., 2005). This suggested that GRIP1b palmitoylation most likely regulates dynamic events such as rapid changes in protein trafficking.

Palmitoylation by DHHC5 targets GRIP1b to dendritic endosomes

Endogenous GRIP1b is highly palmitoylated (Fig 2E), but the signal detected by GRIP1b immunostaining (Fig 2D) does not discriminate between palmitoylated and non-palmitoylated forms of GRIP1b. We therefore sought to compare the neuronal distribution of non-palmitoylated and palmitoylated GRIP1b more directly. Non-palmitoylated GRIP1b was made by mutating the single palmitoylated Cysteine residue, Cys11, to a non-palmitoylatable Serine (GRIP1b-C11S; Fig 3C). To mimic palmitoylation, we added a consensus sequence to the GRIP1b N-terminus that directs addition of myristate (C14, fully saturated), an almost identical lipid to palmitate (C16, fully saturated), which is attached at an almost identical position in the GRIP1b protein (Fig 3C). Importantly, however, myristate modification is irreversible (Johnson et al., 1994), so myristoylated GRIP1b (Myr-GRIP1b) mimics constitutively palmitoylated GRIP1b.

The distribution of GRIP1b-C11S and myr-GRIP1b differed dramatically in hippocampal neurons. While GRIP1b-CS immunofluorescence was restricted to the cell soma and proximal dendrites, myr-GRIP1b immunofluorescence extended far into distal dendrites (Fig 3D, quantified in 3E). Even more dramatically, while GRIP1b-CS immunofluorescence was almost entirely diffuse, Myr-GRIP1b was strikingly punctate (Fig 3D, quantified in 3F).

Similar to endogenous GRIP1b, Myr-GRIP1b puncta were present throughout dendritic shafts, but only rarely present in dendritic spines (Fig S3A, quantified in Fig S3B, S3C). Numerous Myr-GRIP1b puncta were detected far (>60 microns) into distal dendrites, and their size and distribution resembled previously described endogenous GRIP1/GRIP1b puncta, which colocalize with markers for recycling endosomes, but not with early endosome, synaptic or Golgi markers (Mao et al., 2010; Fig S2G, H). Indeed, dendritic Myr-GRIP1b puncta colocalized extensively with Alexa555-Transferrin (Fig 3G), but only rarely with the early endosomal marker EEA1 (Fig S3D), confirming their identity as recycling endosomes. Moreover, live imaging of GFP-tagged Myr-GRIP1b revealed that a subset of these recycling endosomes is highly motile (Movie S1). Together, these data suggest that mimicking N-terminal palmitoylation targets GRIP1b to motile dendritic trafficking endosomes.

PDZ Ligand-dependent palmitoylation by DHHC5 targets GRIP1b to dendritic vesicles

These findings suggested that wild type GRIP1b might distribute between the diffuse pattern of GRIP1b-C11S and the punctate pattern of Myr-GRIP1b. However, dendritic puncta of transfected GRIP1bwt were far less numerous than those seen with Myr-GRIP1b (Fig 3D, F). We hypothesized that this might be due to limiting endogenous DHHC5 PAT activity. Consistent with this notion, transfection of wild type DHHC5 transformed GRIP1bwt distribution in two ways. First, DHHC5wt increased the level of GRIP1bwt detected in distal dendrites (Fig4A, quantitated in 4B). Second, DHHC5wt transformed GRIP1bwt staining from a largely diffuse pattern to one that was strikingly punctate (Fig4A, quantitated in 4C). Indeed, the number of GRIP1bwt puncta in distal dendrites of HA-DHHC5 expressing neurons approached that seen with Myr-GRIP1b. Changes in GRIP1bwt distribution were likely due to direct palmitoylation because HADHHC5wt expression did not affect GRIP1b-C11S distribution. Strikingly, neither DHHS5 nor DHHC5ΔC increased GRIP1b targeting to dendrites (Fig4A–C), despite the normal dendritic targeting of these mutants (Fig S4). Together, these results suggest that palmitoylation by DHHC5 targets GRIP1b to recycling endosomes and that, as in heterologous cells (Fig 1G), this phenotypic effect requires both the PAT activity and PDZ binding ability of DHHC5.

The rapid turnover of palmitate on GRIP1 suggested that GRIP1 vesicular localization might be affected by acute inhibition of palmitoylation. Indeed, acute treatment (90min) with 2-Bromopalmitate dramatically dispersed GRIP1 puncta in both proximal and distal dendrites (Fig 5A). These findings are consistent with palmitoylation reversibly targeting GRIP1b to dendritic endosomes and suggested that palmitoylation might modulate interactions with other GRIP1 partners that control vesicle trafficking. One such trafficking protein is the dendritic kinesin motor protein KIF5, whose interaction with GRIP1 is critical for GluA2 trafficking within dendrites (Setou et al., 2002). We therefore addressed whether GRIP1 palmitoylation might modulate GRIP1 interactions with KIF5, by co-expressing KIF5C with wildtype, non-palmitoylatable or myristoylated GRIP1b in heterologous cells. Strikingly, myristoylated GRIP1 bound more KIF5C than did wildtype GRIP1, while GRIP1b-C11S bound KIF5C only minimally (Fig 5B). Moreover, in neurons, a Myr-GRIP1b mutant lacking the previously reported KIF5-binding domain of GRIP1 (Setou et al., 2002; myr-GRIP1b-delKBD) showed markedly reduced targeting to distal dendrites (Fig 5C). These findings suggest firstly that GRIP1b palmitoylation favors GRIP1b – KIF5 binding, that these interactions act in concert to control GRIP1b dendritic targeting, and may enhance the ability of GRIP1b to bridge vesicular cargoes, particularly glutamate receptors, with dendritic motor proteins.

Membrane-associated GRIP1b accelerates AMPA receptor recycling

GRIP1 regulates AMPA receptor targeting to dendrites and the recycling of AMPA receptors to the plasma membrane following NMDA receptor activation (Setou et al., 2002; Mao et al. 2010). We therefore hypothesized that GRIP1b palmitoylation might in turn affect GRIP1b's ability to regulate AMPA receptor recycling. To address this possibility, we transfected hippocampal neurons with wild type, non-palmitoylatable or constitutively membrane targeted forms of GRIP1b, together with a pHluorin tagged GluA2 AMPA receptor, to which GRIP1 directly binds (Dong et al., 1997; Mao et al., 2010). The pHluorin tag fluoresces brightly at neutral pH, as when the receptor is present on the plasma membrane. Brief treatment with NMDA drives internalization of pHGluA2 to recycling endosomes, whose acidity (pH<6.6) dramatically quenches pHGluA2 fluorescence, while NMDA washout induces pHGluA2 recycling to the plasma membrane and fluorescence recovery (Ashby et al., 2004, Lin and Huganir, 2007; Thomas et al., 2008; Mao et al., 2010; Fig 6A). Fluorescence of pHGluA2 therefore acts as a read-out of receptor distribution and can be used to determine rates and degrees of internalization and recycling. In particular, the half time of fluorescence recovery time (T 1/2), derived from a single exponential fit of the recycling phase, provides a quantitative measure of recycling rate.

In neurons transfected with GRIP1bwt or GRIP1bC11S, rates of pHGluA2 internalization and recycling were highly similar to neurons transfected with vector alone (Fig 6B). However, pHGluA2 recycling was markedly accelerated in neurons transfected with myristoylated GRIP1b (Fig 6C). This accelerated recycling was also seen in neurons transfected with DHHC5, which is predicted to increase palmitoylation of endogenous GRIP1b (Fig 6D, Fig S5A). Both Myr-GRIP1b and DHHC5 caused accelerated recycling of both somatic and dendritic pHGluA2 (Fig 6, Fig S5 B–E). The effect of transfected DHHC5 is likely due to direct palmitoylation of GRIP1b, as although GluA2 is a known palmitoylated protein (Hayashi et al., 2005), it is not detectably palmitoylated by DHHC5 (Fig S5B). AMPA receptor recycling is therefore significantly accelerated under conditions where GRIP1b membrane attachment is enhanced (Fig 6E, Fig S5E). Myr-GRIP1b, which is targeted to trafficking vesicles, also colocalized extensively with pH-GluA2 in dendritic punctae in fixed neurons (Figure S5C), suggesting that effects on trafficking were likely due to a direct GRIP1b-pHGluA2 interaction.

Discussion

Here we report that two PATs use a novel PDZ domain recognition mechanism to palmitoylate and control the distribution and trafficking of GRIP1b. The role of GRIP1b palmitoylation is distinct from that observed for many palmitoyl-proteins: palmitoylation targets GRIP1b to motile trafficking vesicles in neuronal dendrites, and drives accelerated recycling of AMPA-type glutamate receptors. These findings are consistent with both the dendritic localization of the major GRIP1 PAT, DHHC5, and the known role of GRIP1 in the dendritic trafficking of its interacting partners, most notably AMPA-type glutamate receptors (Setou et al., 2002; Mao et al., 2010). Why, though, is palmitoylated GRIP1b not detected at the plasma membrane, as observed for several other palmitoylated proteins? A likely explanation is that the GRIP1b N-terminus lacks a second membrane-targeting signal, such as an additional lipid modification site or a polybasic sequence (Sigal et al., 1994; Dunphy and Linder, 1998; Resh, 2006). 'Two signal' modification of this type is essential for plasma membrane targeting of GFP, while GFP modified with only a single lipid and lacking a polybasic sequence localizes to intracellular vesicles that are most likely endosomes (McCabe and Berthiaume, 2001). The `single signal' present in GRIP1b would therefore be predicted to direct targeting to vesicles. Querying databases for conserved N-terminal Cysteines surrounded by non-basic residues may well reveal further proteins that are targeted to vesicles by palmitoylation.

Several lines of evidence support the conclusion that palmitoylated GRIP1b is targeted to dendritic endosomes; endogenous GRIP1b, which is highly palmitoylated, shows a dendritic distribution very similar to the palmitoylation mimic Myr-GRIP1b. Moreover, DHHC5 targets GRIP1bwt, but not the palmitoylation mutant GRIP1b-C11S, to similar dendritic puncta. Notably, though, the endosomal targeting of palmitoylated GRIP1b is distinct from the synaptic targeting described for the closely related palmitoylated GRIP2b (DeSouza et al., 2002; Misra et al., 2010). Consistent with these reports, we also observed prominent GRIP2b targeting to dendritic spines, which did not require DHHC5 or DHHC8 co-expression (not shown). Although GRIP1 and GRIP2 can compensate for one another in cerebellar Purkinje neurons (Takamiya et al., 2008), two related issues likely underlie the distinct regulation of these two proteins in forebrain. First, plasma membrane / synaptic targeting of GRIP2b is consistent with the additional basic residues that surround the palmitoylated Cysteine at the GRIP2b N-terminus, compared to GRIP1b. Second, while the PDZ domains of GRIP1 and GRIP2 are highly homologous, the KIF5-binding region of GRIP1 (between PDZ6 and PDZ7; Setou et al., 2002) is poorly conserved in GRIP2, suggesting that GRIP1 is unique in its ability to interact with motor proteins that control vesicular cargoes. In further support of their distinct regulation, we also observed no increase in GRIP2b palmitoylation by either DHHC5 or DHHC8 in transfected heterologous cells (not shown), and a much slower GRIP2 palmitoylation turnover rate in neurons, compared to GRIP1b (not shown). Together, these findings suggest that palmitoylated GRIP1b plays a unique role in endosomal trafficking and coupling to kinesin motor proteins.

Our finding that GRIP1b palmitoylation specifically affects activity-dependent AMPA-R recycling would appear to differ from a recent report (Hanley and Henley, 2010), which implicates GRIP1b in NMDA-induced AMPA-R internalization. However, we suspect that experimental differences likely underlie this discrepancy and that our findings more accurately reflect the physiological role of GRIP1b. In particular, Hanley and Henley used Sindbis virus infection to express GRIP1b, a system that has two key issues when used to study intracellular trafficking. First, host cell protein synthesis is shut down, complicating the analysis of intracellular trafficking phenotypes. Second, GRIP1b is over-expressed at high levels, leading to intracellular aggregation (visible in some images from this report (Hanley and Henley, 2010). Moreover, the authors used a large, N-terminal (YFP) tag close to the site of GRIP1b palmitoylation, which may well affect regulation of GRIP1b palmitoylation and/or functional downstream effects that depend on this modification.

We recently developed a more physiological genetic manipulation approach (Mao et al., 2010) to circumvent many issues associated with GRIP1 overexpression. This approach allowed us to reveal a specific role for GRIP1 in activity-dependent recycling of both endogenous and exogenous (pHluorin-tagged) AMPA-Rs. In contrast, we observed no role for GRIP1 on basal or activity-induced AMPA-R internalization. The findings reported here are highly consistent with the report by (Mao et al., 2010) and with recent work from our collaborators (Mejias et al., 2011), again observing a role for GRIP1 in activity-dependent AMPA-R recycling. Moreover, in this study we also deliberately transfected only small amounts of plasmid DNA, expressing GRIP1 from a weak promoter (see Methods) to avoid GRIP1b aggregation. Our GRIP1b constructs carried only a small C-terminal myc tag far from the site of palmitoylation, which is unlikely to interfere with GRIP1b function. Evidence from multiple readouts, using both endogenous and exogenous AMPA-Rs, therefore suggests that the predominant physiological role of GRIP1 is to control activity-dependent AMPA-R recycling, and that palmitoylated GRIP1b enhances this process.

We note that, in addition to GRIP1b described here, their prominent dendritic distribution suggests that DHHC5/8 are well placed to palmitoylate other proteins at or near glutamatergic synapses. Although DHHC5 does not palmitoylate GluA2 (Fig S6B), its

targets may include other AMPA-R subunits (Hayashi et al., 2005), NMDA-Rs (Hayashi et al., 2009) or other PDZ domain adaptor proteins (Fukata and Fukata, 2010), all of which are known to be palmitoylated. Indeed, other DHHC5 substrates may underlie effects that cannot be fully attributed to GRIP1b palmitoylation (e.g. the slightly reduced pHGluA2 fluorescence decrease seen with DHHC5 transfection; Fig 6D). In addition, the presence of transfected DHHC5 in long, aspiny neurites that are likely axons, suggests that DHHC5 may palmitoylate additional axonal / presynaptic substrates in addition to its dendritic regulation of GRIP1b described here.

The identification of additional DHHC5/8 substrates remains an exciting area for future investigation. We note with interest that other PATs cannot compensate for loss of DHHC5/8 to palmitoylate GRIP1 in neurons, and in transfected cells even PATs that display broad substrate specificity (DHHC3, DHHC7; Fukata et al., 2004; Fernandez-Hernando et al., 2006; Greaves et al., 2008; Ponimaskin et al., 2008; Tsutsumi et al., 2009) or preferentially palmitoylate cysteines located close to the N-termini of their substrates (DHHC20; Draper and Smith, 2010) do not palmitoylate GRIP1b (Fig S1). These findings suggest that GRIP1b palmitoylation by DHHC5/8 has distinct requirements, namely that the PDZ domain interaction unique to DHHC5 and DHHC8 is essential to render GRIP1b accessible as a substrate. DHHC5, in particular, is a major GRIP1b PAT in neurons but cannot palmitoylate several other palmitoyl-proteins (Fukata et al., 2004; Fernandez-Hernando et al. 2008; Greaves et al., 2008; Tsutsumi et al., 2009), suggesting that PDZ domain-dependent recognition is a key determinant of DHHC5 substrate specificity.

Multiple studies link DHHC5 and DHHC8 to both normal higher brain function and neuropsychiatric disease (Mukai et al., 2004; Mukai et al., 2008; Li et al., 2010). However, no neuronal substrates have been identified for DHHC5, and although PSD-95 palmitoylation is reduced in DHHC8 knockout mice (Mukai et al., 2008), other PATs are also reported to directly palmitoylate PSD-95 in neurons (Noritake et al., 2009), raising the possibility that this may be an indirect effect. Thus, our identification of GRIP1b as the first bona fide neuronal substrate for DHHC5/8 has broad implications, since GRIP1 is also genetically linked to neuropsychiatric conditions and to autism (Gratacos et al., 2006; Mejias et al., 2011). This raises the possibility that abnormal dendritic and/or synaptic palmitoylation of PDZ domain proteins such as GRIP1 contributes to the pathogenesis of these conditions. Indeed, another PDZ domain protein linked to neuropsychiatric disease is also palmitoylated by DHHC5 and DHHC8 in a PDZ ligand manner (G.M.T., T.H and R.L.H., unpublished). These findings raise the hope that therapeutic targeting of specific PATs and/or their interactions with specific substrates may provide a new approach to better therapeutic treatments for these diseases.

Materials and Methods

Antibodies

The following antibodies, from the indicated sources, were used in this study. Monoclonal antibodies: GRIP1, Fyn, GM130 (BD Biosciences), PSD-95 (K28/43, Neuro mAb), GFP (3E6, Invitrogen), myc, HA11, (Covance), HA F-7 (Santa Cruz). Polyclonal antibodies: DHHC5 (Sigma), ZDHHC8 (Everest Biotech), rabbit anti-HA (QED Bioscience). Antibody against the C-terminus of GRIP1 has been previously described (Dong et al., 1997).An antibody raised against the unique N-terminus of GRIP1b (amino acids 5–19; KKNIPICLQAEEEQER) was affinity purified using the antigenic peptide. Alexa-dye conjugated fluorescent secondary antibodies and Alexa-transferrin were from Invitrogen.

Molecular Biology and cDNA clones

All mammalian DHHC5 and DHHC8 sequences reported share an identical C-terminal 15 amino acids, terminating in a Type II PDZ ligand. A C-terminal 109 amino acid `bait' from human DHHC8 (Ohno et al., 2006) was subcloned into the pPC97 yeast expression vector and used to screen a rat hippocampal cDNA library. Clones that grew on quadruple-deficient plates (Leu-, Trp-, His-, Ade-) were selected, and their plasmids were isolated and sequenced. Positive clones were subcloned into myc-tagged pRK5 mammalian expression vector and C-termini of both DHHC5 and DHHC8 were subcloned into a mammalian GST fusion vector (Thomas et al., 2005) for binding experiments in mammalian cells.

Full length untagged rat GRIP1a and mouse GRIP1b cDNAs in pBK expression vector have been previously described (Dong et al., 1999; Yamazaki et al., 2001). GRIP1b C11S was generated by Quickchange mutagenesis. A myristoylation consensus sequence (MGQSLTT; Wyszinski et al., 2002) was added to the N-terminus of GRIP1b-C11S by PCR to generate Myr-GRIP1b. The myristoylation consensus contains no polybasic sequence that might affect membrane targeting, and Myr-GRIP1b contained a mutated Cys11->Ser, so that only a single lipid modification occurs, as for GRIP1bwt. For live imaging, full length Myr-GRIP1b sequence was amplified by PCR and subcloned into eGFP-N1 vector using NheI and NotI sites. HA-tagged mouse DHHC5 and DHHC8 and mycHis-tagged human DHHC8 cDNA have been previously described (Fukata et al, 2004; Ohno et al., 2006). Catalytically inactive (DHHC -> DHH**S**) and deltaC (ΔC) mutants (lacking the last five amino acids that constitute the PDZ ligand) of DHHC5 and DHHC8 were generated by Quickchange. The previously reported kinesin binding domain (KBD; Setou et al., 2002) of GRIP1b was deleted by Splicing by Overlap Extension (SOE)-based PCR using the Myr-GRIP1b-myc cDNA as template to generate Myr-GRIP1b-myc-deltaKBD.

Lentiviral infection and shRNA knockdown

shRNAs (in vector pLKO; Mission shRNA library) targeting sequences identical in both rat and mouse DHHC5 (5'-CCTCAGATGATTCCAAGAGAT-3') or DHHC8 (5'-CTTCAGTATGGCTACCTTCAT-3') were tested for their ability to reduce expression of HA-tagged DHHC5 and DHHC8 mouse cDNAs in cotransfected HEK293T cells. After confirming that these sequences effectively and specifically suppressed expression of DHHC5 and DHHC8, respectively, each sequence was amplified by PCR, together with its neighboring H1 promoter. The resultant H1-shRNA cassettes were subcloned into the PacI site of the lentiviral FUGW vector (Lois et al., 2002) and verified by sequencing. ShRNA-resistant DHHC5 was generated by mutating five nucleotides within the shRNA target sequence, without altering protein coding. This resultant `rescue' cDNA was amplified by PCR with SalI and NotI primers and inserted into a modified FUGW vector by replacing the GFP cassette with myc-tagged DHHC5.

VSV-G pseudotyped lentivirus was generated by standard methods. Briefly, HEK293T cells were cotransfected with FUGW-shRNA vector and VSV-G and Delta8.9 plasmid cDNAs using a Lipofectamine-based method. Supernatant containing virus was harvested at 48h and 72h post-transfection, concentrated by ultracentrifugation, resuspended in Neurobasal medium and used to infect dissociated neurons at DIV9. Neurons were lysed at DIV16.

Biochemistry

All biochemical experiments were performed at least three times and in each case a representative experiment is shown. Quantified analysis of certain experiments is presented in Supplementary Figures.

Radioactive and non-radioactive palmitoylation assays

[^{3}H]-palmitate labeling of 293T cells and cultured neurons was performed as described (Hayashi et al., 2005; Hayashi et al., 2009). Acyl biotinyl exchange (ABE) assay was performed as described (Hayashi et al., 2009), similar to published protocols (Drisdel and Green, 2006; Wan et al., 2007). For neuronal ABE experiments, neurons were lysed directly in buffer containing 2% SDS and 20 mM methyl-methane thiosulfonate (MMTS, to block free thiols). 2 Bromopalmitate was prepared as a 100 mM stock in ethanol and added to neurons at a final concentration of 100 micromolar. Sister cultures were treated with solvent control (0.1% (v/v) ethanol).

For ABE analysis of forebrain, one mouse (P21) forebrain was homogenized in ice-cold buffer containing 10mM HEPES pH 7.4, 0.32M sucrose, 20mM MMTS and protease inhibitors. Unhomogenized tissue was pelleted by centrifugation at 2,100 × *g* and the supernatant was rapidly warmed to room temperature, adjusted to 1% (w/v; final concentration) SDS, centrifuged at 27,000 × *g* to remove insoluble material, and used for ABE as above.

Transfection

HEK 293T cells were transfected using a calcium phosphate-based method as previously described (Thomas et al., 2005). Neurons were transfected using a lipofectamine-based method and used for live imaging or fixed with paraformaldehyde (see below) either 10–16 hours later (for GRIP1 transfections) or 72 hours later (for pHluorin-GluA2 transfections).

Co-precipitation in HEK293T cells

HEK 293T cells were transfected with pCIS vector constructs to express GST alone, GST fusions of DHHC5 and DHHC8 wild type or deltaC C-termini, plus myc-tagged GRIP456. Cells were lysed in Immunopreciptation buffer (IPB; Thomas et al., 2005) containing protease and phosphatase inhibitors. Insoluble material was pelleted by centrifugation and the supernatants (termed lysates) were incubated with Glutathione Sepharose (GE Healthcare). Beads were washed extensively with IPB, denatured in SDS sample buffer and samples were subjected to SDS-PAGE. Gels were transferred to PVDF membranes and immunoblotted with anti-myc or anti-GST antibodies. For GRIP1-KIF5 binding, each GRIP1 construct, containing a C-terminal myc tag, was co-transfected with HA-tagged KIF5C. Cells were lysed 16 h after transfection and lysates processed as above.

Cultured primary neurons

Cortical neurons were prepared as described (Thomas et al., 2008) and used at DIV16-20. Hippocampal neurons on coverslips were prepared by the method of Goslin and Banker (Goslin and Banker, 1998) for fixed immunostaining of endogenous proteins; or as previously described (Lin et al., 2007) for transfection experiments. Transfection was performed at DIV15–17. All neuronal experiments were performed from the indicated numbers of individual neurons, using at least two different sets of cultures. Pooled data from each condition are plotted as mean ± SEM and statistical significance was determined by t-test or ANOVA.

Immunostaining

Neurons on coverslips were fixed in PBS containing 4% (w/v) sucrose and 4% (w/v) paraformaldehyde. Coverslips were washed with PBS and cells permeabilized with PBS containing 0.25% (w/v) Triton X-100. Following brief washing with PBS, coverslips were blocked overnight at 4 degrees C in 10% Normal goat serum (NGS) diluted in PBS.

Coverslips were then incubated with primary antibodies (diluted in 10% NGS) for 3 hours at room temperature, washed with PBS and incubated with fluorescent conjugated goat-anti-rabbit or goat anti-mouse secondary antibodies. In some experiments, isotype specific (Alexa-conjugated goat anti-mouse IgG1 or goat anti-mouse IgG2a) secondary antibodies were used.

For live cell labeling with Alexa555-transferrin, hippocampal neurons transfected with Myr-GRIP1b-myc as above were incubated for 1h at 37 degrees in recording buffer (Lin and Huganir, 2007), then for 20 minutes at 37 degrees in recording buffer containing 25 μg/ml Alexa555 transferrin. Unbound Alexa555-transferrin was removed by three quick washes in recording buffer, prior to fixation, permeabilization and incubation with anti-myc antibody.

Microscopy and Image Analysis

The majority of neuronal images were acquired using a laser scanning confocal microscope (LSM 510, Zeiss) with a 63× oil immersion Neofluor objective (N.A.1.3, Zeiss). Some images were acquired using a comparable system (Nikon C2 confocal) with a 60× objective (N.A. 1.4, Nikon). For fixed cell imaging, multiple individual sections (1.0 Airy Units, approx. 0.4 micron slices) of a neuron of interest were acquired to capture the entire dendritic tree. A single maximum intensity projection was then generated from these confocal Z-stacks.

Analysis of dendritic puncta and neuronal morphology

Offline image analysis was performed with NIH ImageJ software. To analyze the dendritic distribution of transfected GRIP1, a single maximum intensity projection image was generated. The average somatic fluorescence intensity in the cell body was calculated by manually tracing the soma, using signal from cotransfected GFP to determine morphology. The GFP fill was then used to trace 20 micron segments along the three most prominent dendrites emanating from the cell body. Each dendritic segment was then outlined in the GRIP1-myc channel and the average fluorescence intensity logged to a spreadsheet. The analysis was repeated at 20 micron steps for each image. Similar analysis was performed to determine the dendritic distribution of transfected DHHC5 (wild type and mutants) and DHHC3.

To quantitate dendritic puncta of transfected GRIP1, each dendritic segment (outlined in the GRIP1-myc channel as above) was thresholded by gray value at a level close to 50% of the dynamic range. This threshold value was kept constant for all images in each condition and background noise from these images was negligible. The same dendritic regions were outlined as above, the software was used to count puncta of 2–20 pixel units within each segment, and the results were logged to a spreadsheet. The analysis was repeated at 20 micron steps for each image.

To analyze the effect of 2-Bromopalmitate on endogenous GRIP1 puncta, images were initially thresholded as above. A new image was generated of those puncta that overlapped a GFP-transfected neuron within the same field. This allowed GRIP1 signals to be assigned to dendrites emanating from a specific neuron with a defined center. The soma was traced and masked manually, and the GFP signal was used to trace 20 micron dendritic segments as above. Puncta in each dendritic segment were counted as above and logged to a spreadsheet.

Live imaging of pHluorin-tagged GluA2

Live imaging was performed essentially as described (Lin and Huganir, 2007; Thomas et al., 2008). Briefly, neurons on coverslips were transfected with pH-GluA2 plus vector, GRIP1b

wild type or mutants, or HA-DHHC5. 72 hrs after transfection coverslips were assembled in a chamber perfused with imaging buffer (Lin and Huganir, 2007; Thomas et al., 2008). A single neuron was selected based on pHluorin signal and baseline fluorescence was monitored for 10 minutes prior to perfusion for 5 minutes with 20 micromolar NMDA in low-magnesium imaging buffer (Lin and Huganir, 2007; Thomas et al., 2008) and subsequent recovery in standard imaging buffer. Using ImageJ, the change of pHGluA2 fluorescence in both the cell soma and in a single primary dendrite was monitored and logged to a spreadsheet.

Supplementary Material

Refer to Web version on PubMed Central for supplementary material.

Acknowledgments

We gratefully acknowledge Drs. Masaki and Yuko Fukata (National Institutes of Natural Sciences, Okazaki, Japan) for mouse DHHC cDNAs, and Dr. Y. Igarashi (Hokkaido University, Japan) for human DHHC5 and DHHC8 cDNA. We thank Mrs. Min Dai for neuronal `Banker' cultures, Mr. R. Johnson for the myc-FUW vector and KBD construct, Mrs. L. Hamm for expert technical assistance, Dr. C.-Y. Su (Yale University) for comments on the manuscript, and Dr. V. Anggono and all other Huganir lab members for helpful discussions. This work was supported by funding from the Howard Hughes Medical Institute and the NIH (R01 MH64856).

References

Ashby MC, De La Rue SA, Ralph GS, Uney J, Collingridge GL, Henley JM. Removal of AMPA receptors (AMPARs) from synapses is preceded by transient endocytosis of extrasynaptic AMPARs. J. Neurosci. 2004; 24:5172–5176. [PubMed: 15175386]

Chen WY, Shi YY, Zheng YL, Zhao XZ, Zhang GJ, Chen SQ, Yang PD, He L. Case-control study and transmission disequilibrium test provide consistent evidence for association between schizophrenia and genetic variation in the 22q11 gene ZDHHC8. Hum. Mol. Genet. 2005; 13:2991–2995. [PubMed: 15489219]

Daw MI, Chittajallu R, Bortolotto ZA, Dev KK, Duprat F, Henley JM, Collingridge GL, Isaac JT. PDZ proteins interacting with C-terminal GluR2/3 are involved in a PKC-dependent regulation of AMPA receptors at hippocampal synapses. Neuron. 2000; 28:873–876. [PubMed: 11163273]

DeSouza S, Fu J, States BA, Ziff EB. Differential palmitoylation directs the AMPA receptor-binding protein ABP to spines or to intracellular clusters. J. Neurosci. 2002; 22:3493–3503. [PubMed: 11978826]

Dong H, O'Brien RJ, Fung ET, Lanahan AA, Worley PF, Huganir RL. GRIP: a synaptic PDZ domain-containing protein that interacts with AMPA receptors. Nature. 1997; 386:279–284. [PubMed: 9069286]

Doyle JP, Dougherty JD, Heiman M, Schmidt EF, Stevens TR, Ma G, Bupp S, Shrestha P, Shah RD, Doughty ML, Gong S, Greengard P, Heintz N. Application of a translational profiling approach for the comparative analysis of CNS cell types. Cell. 2008; 135:749–762. [PubMed: 19013282]

Draper JM, Smith CD. DHHC20: a human palmitoyl acyltransferase that causes cellular transformation. Mol Membr Biol. 2010; 27:123–136. [PubMed: 20334580]

Drisdel RC, Alexander JK, Sayeed A, Green WN. Assays of protein palmitoylation. Methods. 2006; 40:127–134. [PubMed: 17012024]

Dunphy JT, Linder ME. Signalling functions of protein palmitoylation. Biochim Biophys Acta. 1996; 1436:245–61. [PubMed: 9838145]

El-Husseini Ael D, Bredt DS. Protein palmitoylation: a regulator of neuronal development and function. Nature Rev. Neurosci. 2002; 3:791–802. [PubMed: 12360323]

El-Husseini, Ael-D.; Schnell, E.; Dakoji, S.; Sweeney, N.; Zhou, Q.; Prange, O.; Gauthier-Campbell, C.; Aguilera-Moreno, A.; Nicoll, RA.; Bredt, DS. Synaptic strength regulated by palmitate cycling on PSD-95. Cell. 2002; 108:849–863. [PubMed: 11955437]

Fallin MD, Lasseter VK, Wolyniec PS, McGrath JA, Nestadt G, Valle D, Liang KY, Pulver AE. Genomewide linkage scan for bipolar-disorder susceptibility loci among Ashkenazi Jewish families. Am J Hum Genet. 2004; 75:204–19. [PubMed: 15208783]

Feng W, Zhng M. Organization and dynamics of PDZ-domain-related supramodules in the postsynaptic density. Nat. Rev. Neurosci. 2009; 10:87–99. [PubMed: 19153575]

Fernandez-Hernando C, Fukata M, Bernatchez PN, Fukata Y, Lin MI, Bredt DS, Sessa WC. Identification of Golgi-localized acyl transferases that palmitoylate and regulate endothelial nitric oxide synthase. J. Cell Biol. 2006; 174:369–377. [PubMed: 16864653]

Fukata M, Fukata Y, Adesnik H, Nicoll RA, Bredt DS. Identification of PSD-95 palmitoylating enzymes. Neuron. 2004; 44:987–996. [PubMed: 15603741]

Fukata Y, Fukata M. Protein palmitoylation in neuronal development and synaptic plasticity. Nat. Rev. Neurosci. 2010; 11:161–175. [PubMed: 20168314]

Goslin, K.; Banker, G. Culturing Nerve Cells. Second Edition. MIT Press; 1998.

Gratacòs M, Costas J, de Cid R, Bayés M, González JR, Baca-García E, de Diego Y, Fernández-Aranda F, Fernández-Piqueras J, Guitart M, et al. Identification of new putative susceptibility genes for several psychiatric disorders by association analysis of regulatory and non-synonymous SNPs of 306 genes involved in neurotransmission and neurodevelopment. Am J Med Genet B Neuropsychiatr Genet. 2009; 150B:808–816. [PubMed: 19086053]

Greaves J, Salaun C, Fukata Y, Fukata M, Chamberlain LH. Palmitoylation and membrane interactions of the neuroprotective chaperone cysteine-string protein. J. Biol. Chem. 2008; 283:25014–25026. [PubMed: 18596047]

Hanley JG. PICK1: a multi-talented modulator of AMPA receptor trafficking. Pharmacol Ther. 2008; 118:152–160. [PubMed: 18353440]

Hayashi T, Rumbaugh G, Huganir RL. Differential regulation of AMPA receptor subunit trafficking by palmitoylation of two distinct sites. Neuron. 2005; 47:709–723. [PubMed: 16129400]

Hayashi T, Thomas GM, Huganir RL. Dual palmitoylation of NR2 subunits regulates NMDA receptor trafficking. Neuron. 2009; 64:213–226. [PubMed: 19874789]

Heiman M, Schaefer A, Gong S, Peterson JD, Day M, Ramsey KE, Suárez-Fariñas M, Schwarz C, Stephan DA, Surmeier DJ, et al. A translational profiling approach for the molecular characterization of CNS cell types. Cell. 2008; 135:738–748. [PubMed: 19013281]

Huang K, El-Husseini A. Modulation of neuronal protein trafficking and function by palmitoylation. Curr Opin Neurobiol. 2005; 15:527–535. [PubMed: 16125924]

Johnson DR, Bhatnagar RS, Knoll LJ, Gordon JI. Genetic and biochemical studies of protein N-myristoylation. Annu. Rev. Biochem. 1994; 63:869–914. [PubMed: 7979256]

Kang R, Wan J, Arstikaitis P, Takahashi H, Huang K, Bailey AO, Thompson JX, Roth AF, Drisdel RC, Mastro R, et al. Neural palmitoyl-proteomics reveals dynamic synaptic palmitoylation. Nature. 2008; 456:904–909. [PubMed: 19092927]

Kim E, Sheng M. PDZ domain proteins of synapses. Nat. Rev. Neurosci. 2004; 5:771–781. [PubMed: 15378037]

Kornau HC, Schenker LT, Kennedy MB, Seeburg PH. Domain interaction between NMDA receptor subunits and the postsynaptic density protein PSD-95. Science. 1996; 269:1737–1740. [PubMed: 7569905]

Lau CG, Zukin RS. NMDA receptor trafficking in synaptic plasticity and neuropsychiatric disorders. Nat. Rev. Neurosci. 2007; 8:413–426. [PubMed: 17514195]

Leitges M, Kovac J, Plomann M, Linden DJ. A unique PDZ ligand in PKCalpha confers induction of cerebellar long-term synaptic depression. Neuron. 2004; 44:585–594. [PubMed: 15541307]

Li Y, Hu J, Höfer K, Wong AM, Cooper JD, Birnbaum SG, Hammer RE, Hofmann SL. DHHC5 interacts with PDZ domain 3 of post-synaptic density-95 (PSD-95) protein and plays a role in learning and memory. J Biol Chem. 2010; 285:13022–13031. [PubMed: 20178993]

Lin DT, Huganir RL. PICK1 and phosphorylation of the glutamate receptor 2 (GluR2) AMPA receptor subunit regulates GluR2 recycling after NMDA receptor-induced internalization. J. Neurosci. 2007; 27:13903–13908. [PubMed: 18077702]

Lois C, Hong EJ, Pease S, Brown E.J and Baltimore, D. Germline transmission and tissue-specific expression of transgenes delivered by lentiviral vectors. Science. 2002; 295:868–872. [PubMed: 11786607]

Magee AI, Gutierrez L, McKay IA, Marshall CJ, Hall A. Dynamic fatty acylation of p21N-ras. EMBO J. 1987; 11:3353–3357. [PubMed: 3322807]

Mansouri MR, Marklund L, Gustavsson P, Davey E, Carlsson B, Larsson C, White I, Gustavson KH, Dahl N. Loss of ZDHHC15 expression in a woman with a balanced translocation t(X;15)(q13.3;cen) and severe mental retardation. Eur J Hum Genet. 2005; 13:970–977. [PubMed: 15915161]

Mao L, Takamiya K, Thomas G, Lin DT, Huganir RL. GRIP1 and 2 regulate activity-dependent AMPA receptor recycling via exocyst complex interactions. Proc Natl Acad Sci. 2010; 107:19038–19043. [PubMed: 20956289]

McCabe JB, Berthiaume LG. N-terminal protein acylation confers localization to cholesterol, sphingolipid-enriched membranes but not to lipid rafts/caveolae. Mol Biol Cell. 2001; 12:3601–3617. [PubMed: 11694592]

Misra C, Restituito S, Ferreira J, Rameau GA, Fu J, Ziff EB. Regulation of synaptic structure and function by palmitoylated AMPA receptor binding protein. Mol Cell Neurosci. 2010; 43:341–352. [PubMed: 20083202]

Mukai J, Lu H, Burt RA, Swor DE, Lai WS, Karayiorgou M, Gogos JA. Evidence that the gene encoding ZDHHC8 contributes to the risk of schizophrenia. Nature Genet. 2004; 36:725–731. [PubMed: 15184899]

Mukai J, Dhilla A, Drew LJ, Stark KL, Cao L, MacDermott AB, Karayiorgou M, Gogos JA. Palmitoylation-dependent neurodevelopmental deficits in a mouse model of 22q11 microdeletion. Nat Neurosci. 2008; 11:1302–1310. [PubMed: 18836441]

Munton RP, Tweedie-Cullen R, Livingstone-Zatchej M, Weinandy F, Waidelich M, Longo D, Gehrig P, Potthast F, Rutishauser D, Gerrits B, et al. Qualitative and quantitative analyses of protein phosphorylation in naive and stimulated mouse synaptosomal preparations. Mol Cell Proteomics. 2007; 6:283–293. [PubMed: 17114649]

Newpher TM, Ehlers MD. Glutamate receptor dynamics in dendritic microdomains. Neuron. 2008; 58:472–497. [PubMed: 18498731]

Noritake J, Fukata Y, Iwanaga T, Hosomi N, Tsutsumi R, Matsuda N, Tani H, Iwanari H, Mochizuki Y, Kodama T, et al. Mobile DHHC palmitoylating enzyme mediates activity-sensitive synaptic targeting of PSD-95. J. Cell Biol. 2009; 186:147–160. [PubMed: 19596852]

Ohno Y, Kihara A, Sano T, Igarashi Y. Intracellular localization and tissue-specific distribution of human and yeast DHHC cysteine-rich domain-containing proteins. Biochim Biophys Acta. 2006; 1761:474–483. [PubMed: 16647879]

Osten P, Khatri L, Perez JL, Köhr G, Giese G, Daly C, Schulz TW, Wensky A, Lee LM, Ziff EB. Mutagenesis reveals a role for ABP/GRIP binding to GluR2 in synaptic surface accumulation of the AMPA receptor. Neuron. 2000; 27:313–325. [PubMed: 10985351]

Ponimaskin E, Dityateva G, Ruonala MO, Fukata M, Fukata Y, Kobe F, Wouters FS, Delling M, Bredt DS, Schachner M, et al. Fibroblast growth factor-regulated palmitoylation of the neural cell adhesion molecule determines neuronal morphogenesis. J. Neurosci. 2008; 28:8897–8907. [PubMed: 18768683]

Raymond FL, Tarpey PS, Edkins S, Tofts C, O'Meara S, Teague J, Butler A, Stevens C, Barthorpe S, Buck G, et al. Mutations in ZDHHC9, which encodes a palmitoyltransferase of NRAS and HRAS, cause X-linked mental retardation associated with a Marfanoid habitus. Am J Hum Genet. 2007; 80:982–7. [PubMed: 17436253]

Resh MD. Use of analogs and inhibitors to study the functional significance of protein palmitoylation. Methods. 2006; 40:191–197. [PubMed: 17012032]

Rocks O, Peyker A, Kahms M, Verveer PJ, Koerner C, Lumbierres M, Kuhlmann J, Waldmann H, Wittinghofer A, Bastiaens PI. An acylation cycle regulates localization and activity of palmitoylated Ras isoforms. Science. 2005; 307:1746–1752. [PubMed: 15705808]

Sabio G, Reuver S, Feijoo C, Hasegawa M, Thomas GM, Centeno F, Kuhlendahl S, Leal-Ortiz S, Goedert M, Garner C, et al. Stress- and mitogen-induced phosphorylation of the synapse-

associated protein SAP90/PSD-95 by activation of SAPK3/p38gamma and ERK1/ERK2. Biochem J. 2004; 380:19–30. [PubMed: 14741046]

Setou M, Seog DH, Tanaka Y, Kanai Y, Takei Y, Kawagishi M, Hirokawa N. Glutamate-receptor-interacting protein GRIP1 directly steers kinesin to dendrites. Nature. 2002; 417:83–87. [PubMed: 11986669]

Shepherd JD, Huganir RL. The cell biology of synaptic plasticity: AMPA receptor trafficking. Annu Rev Cell Dev Biol. 2007; 23:613–643. [PubMed: 17506699]

Sigal CT, Zhou W, Buser CA, McLaughlin S, Resh MD. Amino-terminal basic residues of Src mediate membrane binding through electrostatic interaction with acidic phospholipids. Proc Natl Acad Sci. 1994; 91:12253–12257. [PubMed: 7527558]

Srivastava S, Osten P, Vilim FS, Khatri L, Inman G, States B, Daly C, DeSouza S, Abagyan R, Valtschanoff JG, et al. Novel anchorage of GluR2/3 to the postsynaptic density by the AMPA receptor-binding protein ABP. Neuron. 1999; 21:581–591. [PubMed: 9768844]

Steinberg JP, Takamiya K, Shen Y, Xia J, Rubio ME, Yu S, Jin W, Thomas GM, Linden DJ, Huganir RL. Targeted in vivo mutations of the AMPA receptor subunit GluR2 and its interacting protein PICK1 eliminate cerebellar long-term depression. Neuron. 2006; 49:849–860.

Takamiya K, Mao L, Huganir RL, Linden DJ. The glutamate receptor-interacting protein family of GluR2-binding proteins is required for long-term synaptic depression expression in cerebellar Purkinje cells. J. Neurosci. 2008; 28:5752–5755. [PubMed: 18509036]

Terashima A, Pelkey KA, Rah JC, Suh YH, Roche KW, Collingridge GL, McBain CJ, Isaac JT. An essential role for PICK1 in NMDA receptor-dependent bidirectional synaptic plasticity. Neuron. 2008; 57:872–882. [PubMed: 18367088]

Thomas GM, Rumbaugh GR, Harrar DB, Huganir RL. Ribosomal S6 kinase 2 interacts with and phosphorylates PDZ domain-containing proteins and regulates AMPA receptor transmission. Proc Natl Acad Sci. 2005; 102:15006–15011. [PubMed: 16217014]

Thomas GM, Lin DT, Nuriya M, Huganir RL. Rapid and bi-directional regulation of AMPA receptor phosphorylation and trafficking by JNK. EMBO J. 2008; 27:361–372. [PubMed: 18188153]

Trinidad JC, Specht CG, Thalhammer A, Schoepfer R, Burlingame AL. Comprehensive identification of phosphorylation sites in postsynaptic density preparations. Mol Cell Proteomics. 2006; 5:914–922. [PubMed: 16452087]

Trinidad JC, Thalhammer A, Specht CG, Lynn AJ, Baker PR, Schoepfer R, Burlingame AL. Quantitative analysis of synaptic phosphorylation and protein expression. Mol Cell Proteomics. 2008; 7:684–696. [PubMed: 18056256]

Tsutsumi R, Fukata Y, Noritake J, Iwanaga T, Perez F, Fukata M. Identification of G protein alpha subunit-palmitoylating enzyme. Mol. Cell. Biol. 2009; 29:435–447. [PubMed: 19001095]

Wan J, Roth AF, Bailey AO, Davis NG. Palmitoylated proteins: purification and identification. Nat. Protoc. 2007; 2:1573–1584. [PubMed: 17585299]

Webb Y, Hermida-Matsumoto L, Resh MD. Inhibition of Protein Palmitoylation, Raft Localization, and T Cell Signaling by 2-Bromopalmitate and Polyunsaturated Fatty Acids. J. Biol. Chem. 2000; 275:261–270. [PubMed: 10617614]

Wyszynski M, Valtschanoff JG, Naisbitt S, Dunah AW, Kim E, Standaert DG, Weinberg R, Sheng M. Association of AMPA receptors with a subset of glutamate receptor-interacting protein in vivo. J Neurosci. 1999; 19:6528–6537. [PubMed: 10414981]

Wyszynski M, Kim E, Dunah AW, Passafaro M, Valtschanoff JG, Serra-Pagès C, Streuli M, Weinberg RJ, Sheng M. Interaction between GRIP and liprin-alpha/SYD2 is required for AMPA receptor targeting. Neuron. 2002; 34:39–52. [PubMed: 11931740]

Yamazaki M, Fukaya M, Abe M, Ikeno K, Kakizaki T, Watanabe M, Sakimura K. Differential palmitoylation of two mouse glutamate receptor interacting protein 1 forms with different N-terminal sequences. Neurosci Lett. 2001; 304:81–84. [PubMed: 11335060]

Zhang FL, Casey PJ. Protein prenylation: molecular mechanisms and functional consequences. Annu. Rev. Biochem. 1996; 65:241–269. [PubMed: 8811180]

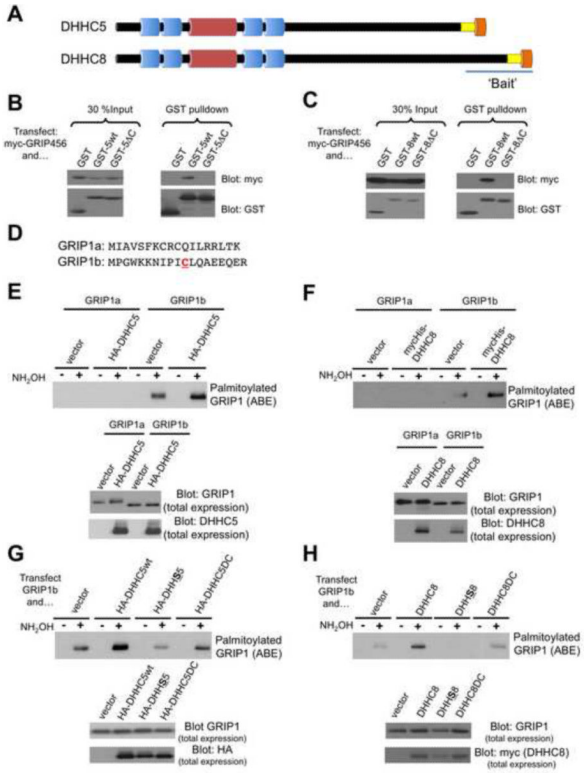

Figure 1. DHHC5 and DHHC8 specifically bind and palmitoylate GRIP1

A: Schematic of the structure of DHHC5 and DHHC8, showing predicted transmembrane domains (blue), catalytic DHHC-Cysteine Rich Domain (red) and identical C-terminal 15 AA sequence (yellow) terminating in identical PDZ ligand (EISV: orange). The region of the DHHC8 C-terminus used as bait for yeast two-hybrid screening is indicated. ***B***: HEK293T cells were transfected with myc-tagged GRIP1-PDZ domains 4 thru 6, together with either GST alone (GST), a GST fusion of the C-terminus of DHHC5 (GST-5wt), or a GST fusion of the C-terminus of DHHC5 lacking the C-terminal PDZ-binding motif (GST-5ΔC). Inputs (left panels) and GST pulldowns (right panels) were immunoblotted with anti-myc and anti-GST antibodies. ***C***: same as ***B***, except that indicated constructs of DHHC8 were cotransfected. ***D***: Comparison of N-terminal sequences of GRIP1a and GRIP1b. The unique Cysteine11 of GRIP1b is reported to be palmitoylated in heterologous cells, but the PAT was not identified. ***E:*** HEK293T cells were transfected with HA-tagged DHHC5 and either full-length untagged GRIP1a or GRIP1b. Acyl-biotin exchange (ABE) was performed to isolate palmitoylated proteins and GRIP1 levels in ABE samples were detected by immunoblotting (top panel). Cell lysates were blotted to detect total levels of GRIP1 (middle panel) and HA-DHHC5 (lower panel). Note that palmitoylated GRIP1 signal is only detected following treatment with hydroxylamine (NH_2OH), an essential step of the ABE reaction. ***F:*** as ***E***, except that cells were transfected with mycHis-DHHC8 and either GRIP1a or GRIP1b and lysates were blotted to detect total levels of GRIP1 (middle panel) and mycHis-DHHC8 (lower panel). ***G:*** Palmitoylation of GRIP1b by DHHC5 requires catalytic activity and PDZ binding ability. HEK293T cells were transfected with GRIP1b plus either empty vector, HA-tagged DHHC5 wild-type (HA-DHHC5wt), catalytically inactive mutant (HA-DHH**S**5) or PDZ ligand mutant (HA-DHHC5ΔC). Lysates were subjected to acyl-biotinyl exchange (ABE) and immunoblotted to detect palmitoylated GRIP1 (upper panel), GRIP1 expression (middle panel) and DHHC5 expression (lower panel). ***H:*** as ***G***, except that cells were transfected with GRIP1b plus either DHHC8wt,

DHHS8 or DHHC8ΔC as indicated. See also Supplemental Figure S1 for additional control experiments and quantified data.

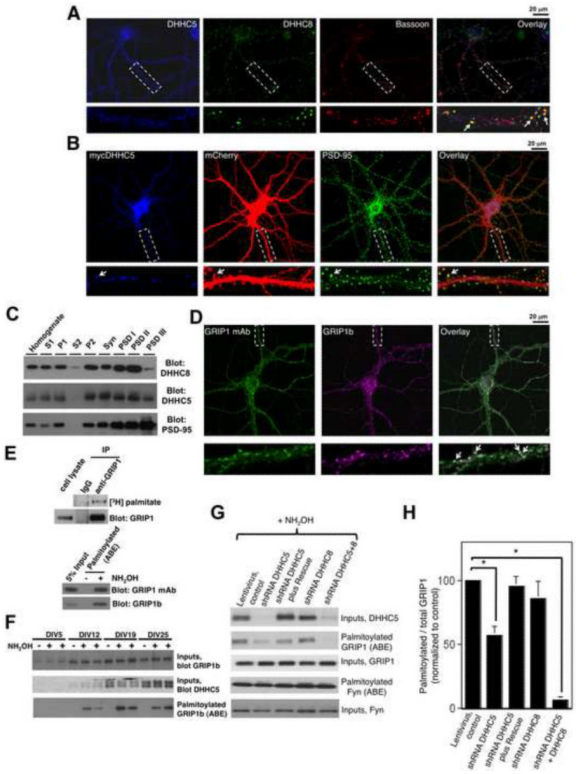

Figure 2. DHHC5/8 control GRIP1 palmitoylation in primary neurons

A: Top row panels: Primary hippocampal neurons were immunostained with antibodies against endogenous DHHC5 (first panel), DHHC8 (second panel) and the synaptic marker Bassoon (third panel). Lower panels show high magnification images of a single highlighted dendrite. Examples of colocalized DHHC8 and Bassoon puncta are indicated with arrows in the overlaid image. A scale bar (20 μm) is marked in this and subsequent images. ***B:*** Immunostaining of primary hippocampal neurons cotransfected with myc-tagged DHHC5 and the soluble marker mCherry, and immunostained for the synaptic marker PSD-95 plus myc and dsRed antibodies. Lower panels show high magnification images of dendrites. An example of myc-DHHC5 colocalized with a PSD-95-positive dendritic spine is shown (arrow) but myc-DHHC5 is more frequently found in dendritic shafts. ***C:*** Equal protein amounts of the indicated subcellular fractions were immunoblotted with DHHC5 or DHHC8 antibodies. Fidelity of the preparation was confirmed by immunoblotting with PSD-95 antibody. ***D:*** Dendritic GRIP1 puncta frequently contain the GRIP1b isoform. Hippocampal neurons were immunostained with GRIP1 monoclonal and GRIP1b-specific polyclonal antibodies as indicated. Lower panels show high magnification images of dendrites. GRIP1 dendritic puncta that are GRIP1b-positive are indicated with arrows in the overlaid image. ***E:*** High stoichiometry of GRIP1b palmitoylation in primary neurons and whole brain. Top panels: Cultured neurons metabolically labeled with [^{3}H]-palmitate were lysed and immunoprecipitated with the indicated antibodies. [^{3}H] signal (upper panel) and GRIP1 protein levels (lower panel) are shown. Bottom panels: Cultured neurons were subjected to ABE and immunoblotted with pan-GRIP1 (upper panel) or GRIP1b-specific antibodies (lower panel). ***F:*** Lysates from cortical neurons cultured for the indicated number of days *in vitro* (DIV) were immunoblotted for expression of GRIP1b (top panel) or DHHC5 (second panel). Lysates subjected to ABE were blotted to detect palmitoylated GRIP1b (bottom panel). ***G:*** Cortical cultured neurons were infected with the indicated lentiviruses containing shRNA sequences to knock down expression of DHHC5, DHHC8 or both PATs. A fraction

of each lysate was immunoblotted to detect total levels of DHHC5 (top panel), GRIP1 (third panel) and Fyn (fifth panel). The remaining lysate was subjected to ABE to detect palmitoylated GRIP1 (second panel) and Fyn (fourth panel). ***H:*** Quantitation of multiple experiments confirms that DHHC5 knockdown significantly reduces GRIP1 palmitoylation (56.8 ± 7.2% of control virus, n=8, $p<0.05$ compared to control virus (FUGW) alone, t-test), shRNA-resistant DHHC5 (`rescue') restores GRIP1 palmitoylation levels (95.5 ± 7.5% of control virus, n=8, not significant from FUGW alone) and GRIP1 palmitoylation is almost completely eliminated by knockdown of both DHHC5 and DHHC8 (6.9 ± 2.6% of control virus, n=3, $p<0.05$ compared to FUGW alone, t-test). See also Supplemental Figure S2.

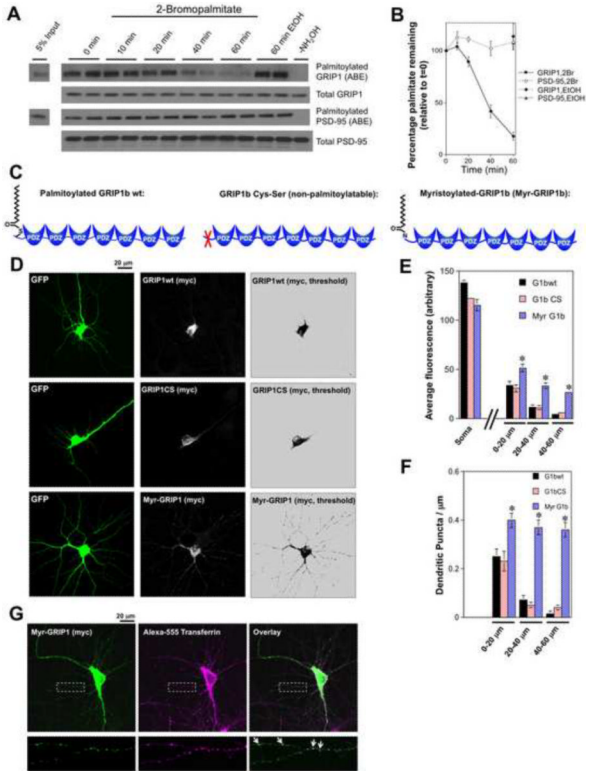

Figure 3. Palmitoylation targets GRIP1b to specific dendritic endosomal vesicles

A: Primary neurons were treated with 100 μM 2-Bromopalmitate for the indicated times or with 0.1% (v/v) EtOH (solvent control). ABE reactions were performed to detect palmitoylated and total levels of GRIP1 and PSD-95, as indicated. ***B:*** Quantitation of palmitate turnover from multiple experiments as in *A*, plotted as Mean ± SEM for n=4 determinations per time point. ***C:*** Schematic of palmitoylated GRIP1b wild type, compared to non-palmitoylatable (GRIP1b-C11S) and constitutive palmitolyation-mimic (G1b-Myr). The Myristoylation consensus adds a similar lipid (C14, saturated) at amino acid 2 (Gly), following cleavage of the initiating Methionine. ***D–F:*** Dendritic targeting of GRIP1b by lipid modification. Representative images of primary hippocampal neurons transfected with GFP as a morphology marker, plus either GRIP1bwt-myc (GRIP1wt, top row), GRIP1b-C11S-myc (GRIP1CS, middle row) or myristoylated GRIP1b-myc (Myr-GRIP1, bottom row), following fixation and staining with antibodies against GFP (first column) and myc (second column). The right column shows myc signals, thresholded at an identical value for each transfected neuron. ***E:*** Quantitation of average fluorescence in cell soma and in dendritic segments at the indicated distances from the soma, in neurons expressing GRIP1bwt-myc (n=14), GRIP1b-C11S-myc (n=16) or myristoylated GRIP1b-myc (n=15). Asterisks indicate significant difference ($p<0.05$) from GRIP1bwt. ***F:*** Number of GRIP1b puncta per dendritic segment for each neuron from E (plotted for 3 dendrites each from n=14, n=16 and n=15 neurons) at the indicated distances from the cell soma. ***G:*** Mimicking palmitoylation targets GRIP1b to recycling endosomes. Myr-GRIP1b-myc transfected neurons were live labeled with Alexa555-transferrin, fixed and stained with anti-myc antibodies. Lower panels show high magnification images of an individual dendrite. Extensively colocalized dendritic puncta are indicated with white arrows in the overlaid image. See also Supplemental Figure S3.

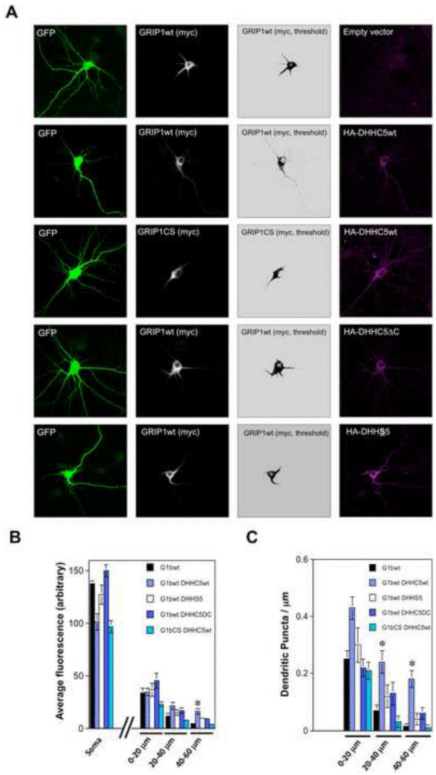

Figure 4. Catalytic activity and PDZ domain recognition by DHHC5 target GRIP1bwt to dendritic vesicles

A: Representative images of primary hippocampal neurons transfected with GFP as a morphology marker, GRIP1bwt-myc or GRIP1b-C11S-myc and either empty vector, HA-DHHC5wt, HA-DHH**S**5 or DHHC5deltaC, following fixation and staining with antibodies against GFP (first column), myc (second column) and HA tags (fourth panels). The third column shows myc signal, thresholded at an identical value for each transfected neuron. ***B:*** Average fluorescence intensity of GRIP1b-myc was plotted as in Fig 3E for GRIP1bwt-myc (n=14), GRIP1bwt-myc plus HA-DHHC5wt (n=19), GRIP1bC11S plus HA-DHHC5wt (n=12), GRIP1bwt plus HA-DHH**S**5 (n=15) and GRIP1bwt plus HA-DHHC5ΔC (n=14). ***C:*** Dendritic puncta of GRIP1b-myc were counted as in Fig 3F. Data for GRIP1bwt-myc from Figure 3 are re-plotted in panels 4B and 4C. Asterisks indicate significant difference ($P<0.05$, t-test) from GRIP1bwt alone. N.B. Quantitative analysis of DHHC5 dendritic distribution confirmed that DHHC5 mutants target equally well, if not better than, DHHC5wt to distal dendrites (See also Supplemental Figure S4), thus impaired targeting does not account for their inability to regulate GRIP1bwt distribution.

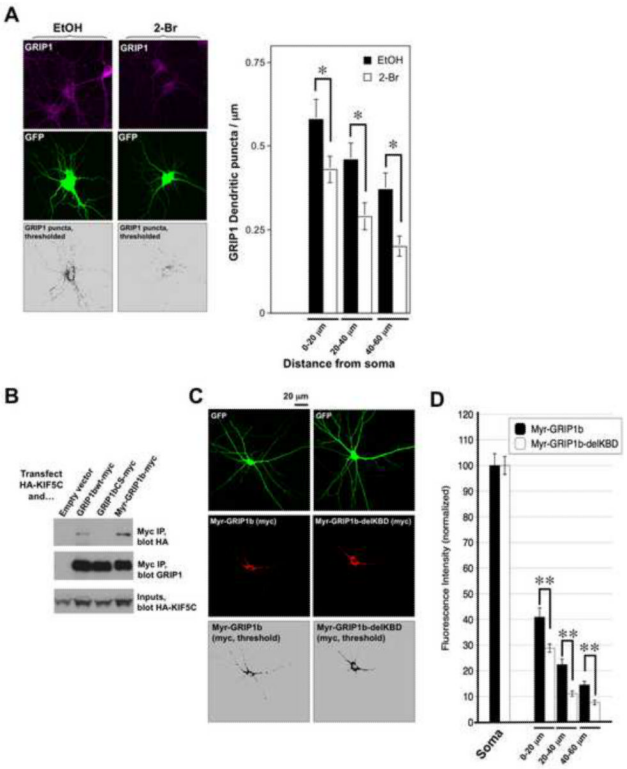

Figure 5. Rapid turnover of palmitate on GRIP1 modulates dendritic targeting

A: Acute treatment with 2-Bromopalmitate disperses dendritic GRIP1 puncta. Top panels: Unprocessed images of GRIP1 immunostaining in GFP-transfected hippocampal neurons. Middle panels: GFP signal (morphology marker to outline individual dendrites). Lower panels: Thresholded puncta within the boundary of an individual GFP-transfected neuron following treatment with EtOH vehicle or 100 μM 2-Bromopalmitate for 90 minutes. Right panel: Plot of number of endogenous GRIP1 puncta (mean ± SEM) counted at indicated distances from the cell soma for 3 dendrites per cell from n=19 cells (control) and n=21 cells (2-Br). ***B:*** Membrane-associated GRIP1b preferentially binds dendritic kinesin KIF5C in heterologous cells. HEK293 cells were transfected with HA-tagged KIF5C plus the indicated myc-tagged GRIP1 constructs. Myc immunoprecipitates were immunoblotted for co-immunoprecipitated HA-KIF5C. ***C:*** Deletion of Kinesin-binding-domain (KBD) impairs Myr-GRIP1b dendritic targeting. Top panels: representative images of primary hippocampal neurons transfected with GFP as a morphology marker, plus either full length myristoylated GRIP1b-myc (Myr-GRIP1b) or Myr-GRIP1b lacking KBD (Myr-GRIP1b-delKBD), following fixation and staining with antibodies against GFP (first row) and myc (second row). The bottom row shows myc signals, thresholded at an identical value for each transfected neuron. ***D:*** Average fluorescence intensity of myc-tagged constructs in soma and dendrites, plotted as in Fig 3E for Myr-GRIP1b (n=13) and Myr-GRIP1b-delKBD (n=12). Double Asterisks indicate significant differences ($p<0.01$, t-test) between conditions at all distances from soma.

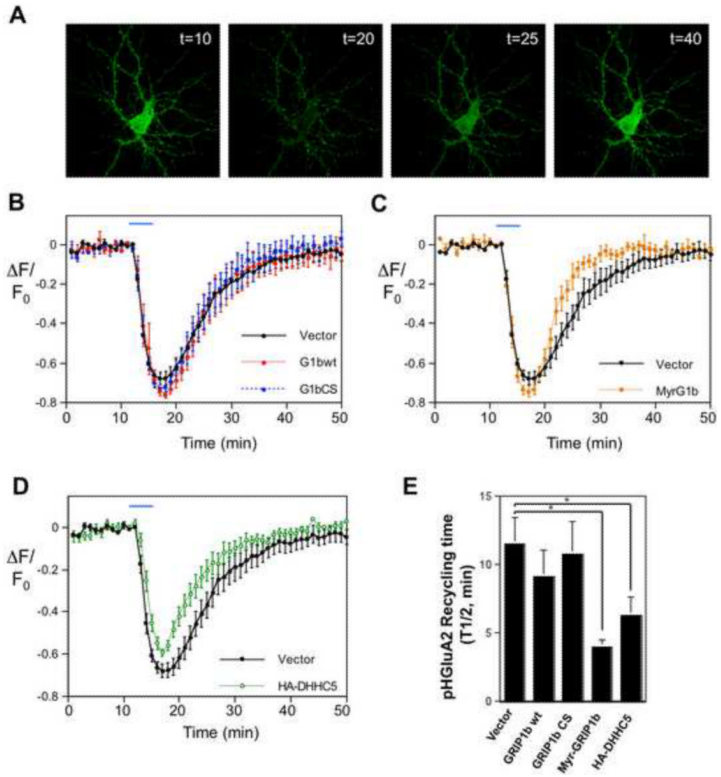

Figure 6. Targeting GRIP1b to membranes increases activity-dependent GluA2 recycling

A: Representative images of fluorescence change of a hippocampal neuron expressing pH-GluA2, exposed at *t*=10 to 20 μM NMDA for 5 min and then allowed to recover following NMDA washout. ***B:*** Fluorescence change (mean ± s.e.m.) during initial incubation, perfusion at *t*= 10 min with 20 μM NMDA for 5 min (blue bar) and washout, plotted for hippocampal neurons transfected with pHluorin-tagged GluA2 (pHGluA2) plus either empty vector (black circles, n=11), myc-tagged GRIP1b wildtype (G1bwt, red circles, n=5) or GRIP1b-C11S (G1bCS, blue circles, n=7). ***C, D:*** As *B*, but for neurons transfected with pH-GluA2 plus myristoylated GRIP1b (Myr-G1b, orange circles, n=6), or with HA-tagged DHHC5 (green circles, n=8), respectively. Recycling in DHHC5-transfected neurons is still accelerated when the fluorescence decrease is scaled to match vector controls (Fig S5A). ***E:*** Time constants (T1/2) of fluorescence recovery, plotted as mean ± SEM for the curves in *B–D*. Asterisks indicate significant difference from pHGluA2 alone ($P<0.05$, t test). See also Supplemental Figure S5.